Table 1 **Predictions of food web models**

c	η_{Cascade}	η_{Niche}	$\eta^{0}_{\text{Webworld}}$	$\eta^{\infty}_{\text{Webworld}}$	$c^{\infty}_{\text{Webworld}}$
0.005	1.12	1.03	1.83	1.61	0.08
0.01	1.09	1.04	1.51	1.20	0.10
0.05	1.08	1.06	1.33	1.11	0.12
0.1	1.06	1.08	1.22	1.09	0.18
0.3	1.04	1.07	1.18	1.07	0.37
0.5	1.01	1.04	1.05	1.04	0.50

The value of the exponent η (the error is always about 0.02) in different models is shown as a function of the connectance c. In static (Cascade[3] and Niche[24]) models the exponent (η_{Cascade} or η_{Niche}) is determined by a single tuning parameter related to c. In the Webworld model[23], a competition parameter tunes the initial state (characterized by the initial values c and $\eta^{0}_{\text{Webworld}}$). Then the model evolves and reaches an 'asymptotic' state characterized by a smaller exponent $\eta^{\infty}_{\text{Webworld}}$ and by a larger connectance $c^{\infty}_{\text{Webworld}}$ (both efficiency and stability increase; see the text). All webs have 1,000 species initially.

former determine the tree structure related to the efficiency of the webs, and the latter form the loops involved in network robustness. Whereas the different nature of the interactions affects the number of loops[29] (and hence the stability), the structure of the spanning trees seems to be invariant and universal. Correspondingly, although the stability properties are likely to be determined by different evolutionary processes, the efficiency of food webs might be the result of a common organizing principle. □

Methods

To define the minimal spanning tree, we discuss two different approaches. One possibility is considering the spanning tree defined by the collection of the shortest chains from the environment to every species (the number of links in these chains gives the trophic level[1–3] of the species). If several spanning trees are still compatible with this prescription, we consider all of them and then perform an ensemble average (see below). Alternatively, we can select for each species the strongest chain from the environment; that is, the one delivering most resources to the species. We prefer to adopt the former definition to include a larger number of data sets in the analysis and to compare them with the models, which in most cases ignore link strength. However, we note that the chains obtained by the two criteria (minimizing chain lengths and maximizing chain strengths) are related. Generally, the transfer of resources along each link is 'inefficient' (only a small fraction of resources is transferred from prey to predator[1,2]) and hence long chains are likely to be weaker than short ones[1]. This argument is also consistent with the empirical observation[2] that only a fraction $\lambda = 0.1$ (known as the ecological efficiency) of the resources of the species in a trophic level is transferred to predators. However, we stress that our definition of 'weak' and 'strong' links does not necessarily reflect the actual link strength.

To obtain the spanning tree minimizing chain length, we first order the species in levels (labelled by $l = 0,1,\ldots,l_{\max}$). Conventionally, the environment belongs to level $l = 0$. All species preying on species at level l (but not at lower ones) belong to level $l + 1$. We then remove all the 'weak' links pointing from a species at a given level l_1 to a species at a level l_2 lower than or equal to l_1. At this point, if each species is left with only one incoming link, the spanning tree is already obtained (all remaining links are 'strong') and the quantities A_i and C_i are directly computed and plotted. Otherwise, if some species still have more than one incoming link, we consider the ensemble of all possible spanning trees (each defined by a different set of 'strong' links) and compute the quantities A_i and C_i on each of them separately. Finally, for each value of A, the average of the corresponding values of C is computed and plotted as a function of A. This produces the curves shown in Fig. 2a–g. The point (A_0,C_0) is the same for every tree in the ensemble of possible ones. The point (1,1) always occurs as a finite-size effect (it corresponds to the 'leaves', where the tree stops branching) together with the point (2,3) independently of the large-scale behaviour of the scaling relations (see Fig. 1). A power-law exactly crossing both points would then miss all other points, unless the value of the exponent were 2. We therefore always exclude the point (1,1) from the fit to avoid forcing the exponent towards an artificially high value. We finally obtain the composite figure (Fig. 2h) by simply plotting together the points (A_0,C_0) of each of the previous panels plus the three additional webs described in the text (we recall that these points are independent of the specific spanning tree realization). The value of C_0 corresponding to $A_0 = 82$ is an average of the values of Silwood Park and Ythan Estuary without parasites (both webs have 81 trophic species).

Received 25 July 2002; accepted 20 March 2003; doi:10.1038/nature01604.

1. Lawton, J. H. in *Ecological Concepts* (ed. Cherret, J. M.) 43–78 (Blackwell Scientific, Oxford, 1989).
2. Pimm, S. L. *Food Webs* (Chapman & Hall, London, 1982).
3. Cohen, J. E., Briand, F. & Newman, C. M. *Community Food Webs: Data and Theory* Biomathematics 20 (Springer, Berlin, 1990).
4. Strogatz, S. H. Exploring complex networks. *Nature* **410,** 268–276 (2001).
5. Albert, R. & Barabási, A.-L. Statistical mechanics of complex networks. *Rev. Mod. Phys.* **74,** 47–97 (2002).
6. Cohen, J. E. *Ecologists' Co-Operative Web Bank 1.00* (The Rockfeller Univ., New York, 1989).
7. Goldwasser, L. & Roughgarden, J. Construction and analysis of a large Caribbean food web. *Ecology* **74,** 1216–1233 (1993).
8. Christian, R. R. & Luczkovich, J. J. Organizing and understanding a winter's seagrass foodweb network through effective trophic levels. *Ecol. Mod.* **117,** 99–124 (1999).
9. Martinez, N. D., Hawkins, B. A., Dawah, H. A. & Feifarek, B. P. Effects of sampling effort on the characterization of food web structure. *Ecology* **80,** 1044–1055 (1999).
10. Memmott, J., Martinez, N. D. & Cohen, J. E. Predators, parasitoids and pathogens: species richness, trophic generality and body sizes in a natural web. *J. Anim. Ecol.* **69,** 1–15 (2000).
11. Hall, S. J. & Raffaelli, D. Food web patterns: lessons from a species-rich web. *J. Anim. Ecol.* **60,** 823–842 (1991).
12. Martinez, N. D. Artifacts or attributes? Effects of resolution on the Little Rock Lake food web. *Ecol. Monogr.* **61,** 367–392 (1991).
13. Huxham, M., Beaney, S. & Raffaelli, D. Do parasites reduce the chances of triangulation in a real food web? *Oikos* **76,** 284–300 (1996).
14. Polis, G. A. Complex trophic interactions in deserts: an empirical critique of food web theory. *Am. Nat.* **138,** 123–155 (1991).
15. Warren, P. H. Spatial and temporal variation in the structure of a freshwater food web. *Oikos* **55,** 299–311 (1989).
16. Montoya, J. M. & Solé, R. V. Small world patterns in food webs. *J. Theor. Biol.* **214,** 405–412 (2002).
17. Williams, R. J., Berlow, E. L., Dunne, J. A. & Barabási, A.-L. Two degrees of separation in complex food webs. *Proc. Natl Acad. Sci. USA* **99,** 12913–12916 (2002).
18. Camacho, J., Guimerà, R. & Amaral, L. A. N. Robust patterns in food web structure. *Phys. Rev. Lett.* **88,** 228102 (2002).
19. Dunne, J. A., Williams, R. J. & Martinez, N. D. Food-web structure and network theory: the role of connectance and size. *Proc. Natl Acad. Sci. USA* **99,** 12917–12922 (2002).
20. Banavar, J. R., Maritan, A. & Rinaldo, A. Size and form in efficient transportation networks. *Nature* **399,** 130–132 (1999).
21. West, G. B., Brown, J. H. & Enquist, B. J. A general model for the origin of allometric scaling laws in biology. *Science* **276,** 122–126 (1997).
22. West, G. B., Brown, J. H. & Enquist, B. J. The fourth dimension of life: fractal geometry and allometric scaling of organisms. *Science* **284,** 1677–1679 (1999).
23. Caldarelli, G., Higgs, P. G. & McKane, A. J. Modelling coevolution in multispecies communities. *J. Theor. Biol.* **193,** 345–358 (1998).
24. Williams, R. J. & Martinez, N. D. Simple rules yield complex food webs. *Nature* **404,** 180–183 (2000).
25. Rodriguez-Iturbe, I. & Rinaldo, A. *Fractal River Basins: Chance and Self-Organization* (Cambridge Univ. Press, Cambridge, 1996).
26. McMahon, T. A. & Bonner, J. T. *On Size and Life* (Scientific American Library, New York, 1983).
27. Martinez, N. D. Constant connectance in community food webs. *Am. Nat.* **139,** 1208–1218 (1992).
28. Dunne, J. A., Williams, R. J. & Martinez, N. D. Network structure and biodiversity loss in food webs: robustness increases with connectance. *Ecol. Lett.* **5,** 558–567 (2002).
29. Cousins, S. H. Species diversity measurements: choosing the right index. *Trends Ecol. Evol.* **6,** 190–192 (1991).
30. Drossel, B., Higgs, P. G. & McKane, A. J. The influence of predator–prey population dynamics on the long-term evolution of food web structure. *J. Theor. Biol.* **208,** 91–107 (2001).

Acknowledgements We acknowledge support from the FET Open Project IST-2001-33555 COSIN.

Competing interests statement The authors declare that they have no competing financial interests.

Correspondence and requests for materials should be addressed to G.C. (gcalda@pil.phys.uniroma1.it).

Defective membrane repair in dysferlin-deficient muscular dystrophy

Dimple Bansal*, Katsuya Miyake†, Steven S. Vogel‡, Séverine Groh*, Chien-Chang Chen*, Roger Williamson§, Paul L. McNeil† & Kevin P. Campbell*

** Howard Hughes Medical Institute, Department of Physiology and Biophysics and Department of Neurology, University of Iowa Roy J. and Lucille A. Carver College of Medicine, Iowa City, Iowa 52242, USA*
† Department of Cellular Biology and Anatomy, The Medical College of Georgia, Augusta, Georgia 30912, USA
‡ Laboratory of Molecular Physiology, National Institute of Alcohol Abuse and Alcoholism, National Institutes of Health, Rockville, Maryland 20852, USA
§ Department of Obstetrics and Gynecology, University of Iowa College of Medicine, Iowa City, Iowa 52242, USA

Muscular dystrophy includes a diverse group of inherited muscle diseases characterized by wasting and weakness of skeletal muscle[1]. Mutations in dysferlin are linked to two clinically distinct muscle diseases, limb-girdle muscular dystrophy type 2B and Miyoshi myopathy, but the mechanism that leads to

© 2003 Nature Publishing Group

muscle degeneration is unknown[2,3]. Dysferlin is a homologue of the *Caenorhabditis elegans fer-1* gene, which mediates vesicle fusion to the plasma membrane in spermatids[4]. Here we show that dysferlin-null mice maintain a functional dystrophin–glycoprotein complex but nevertheless develop a progressive muscular dystrophy. In normal muscle, membrane patches enriched in dysferlin can be detected in response to sarcolemma injuries. In contrast, there are sub-sarcolemmal accumulations of vesicles in dysferlin-null muscle. Membrane repair assays with a two-photon laser-scanning microscope demonstrated that wild-type muscle fibres efficiently reseal their sarcolemma in the presence of Ca^{2+}. Interestingly, dysferlin-deficient muscle fibres are defective in Ca^{2+}-dependent sarcolemma resealing. Membrane repair is therefore an active process in skeletal muscle fibres, and dysferlin has an essential role in this process. Our findings show that disruption of the muscle membrane repair machinery is responsible for dysferlin-deficient muscle degeneration, and highlight the importance of this basic cellular mechanism of membrane resealing in human disease.

To explore the function of dysferlin in skeletal muscle, dysferlin-null mice were generated by homologous recombination. The targeting vector was designed to carry an approximately 12-kilobase deletion at the 3′ end of the gene, deleting the last three coding exons including the transmembrane domain (Supplementary Fig. 1). The genotypes of the mice were verified by PCR (Fig. 1a). The complete loss of protein expression was confirmed by western blot analysis of skeletal muscle microsomes (Fig. 1b). Immunofluorescence analysis revealed localization of dysferlin in both sarcolemma and cytoplasmic vesicles in wild-type muscle as reported previously[5], but no staining was observed in dysferlin-null muscle (Fig. 1c, top row). Dysferlin has been associated with calpain 3 and caveolin-3, mutations of which are responsible for limb-girdle muscular dystrophy type 2A (LGMD2A) and LGMD1C, respectively[1], although the nature of this association remains unclear[6,7]. However, no changes were observed in caveolin-3 (Fig. 1b, c) or calpain 3 (Fig. 1b) expression in dysferlin-null muscle.

Histological and other observations of the skeletal muscle revealed that dysferlin-null mice develop a slowly progressive muscular dystrophy (Fig. 2a). By the age of 2 months, a few individual necrotic and centrally nucleated fibres could be detected throughout the muscle; the number increased with age. By 8 months, the muscle had developed all the pathological characteristics of muscular dystrophy such as regenerating fibres, split fibres, muscle necrosis with macrophage infiltration and fat replacement. Although all the examined muscles showed muscle pathology, the severity of the pathology varied in different muscles of dysferlin-null mice (Supplementary Fig. 2). Plasma membrane disruptions were identified with Evans blue, a membrane-impermeant dye. Unlike dystrophin–glycoprotein complex (DGC)-linked muscular dystrophies, in which clusters of Evans-blue-positive fibres are observed[8,9], dysferlin-null mice showed individual positive fibres, suggesting that the injury and the disease progression take place at the level of single muscle fibres (Fig. 2b). Consistent with the Evans blue analysis was the observation that serum creatine kinase levels of dysferlin-null mice ($1{,}022 \pm 368\ U\,l^{-1}$, mean ± s.d., $n = 8$) were severalfold higher than those of wild-type mice ($157 \pm 84\ U\,l^{-1}$, $n = 5$). Muscle regeneration is a response to muscle degeneration commonly seen in muscular dystrophy. A muscle undergoing active regeneration has centrally nucleated muscle fibres and large variability in fibre size. About 10% of all fibres in dysferlin-null muscle were centrally nucleated by 2 months of age, 20% by 4 months and 48% and 65% by 8 and 10 months, respectively (Fig. 2c). Centrally

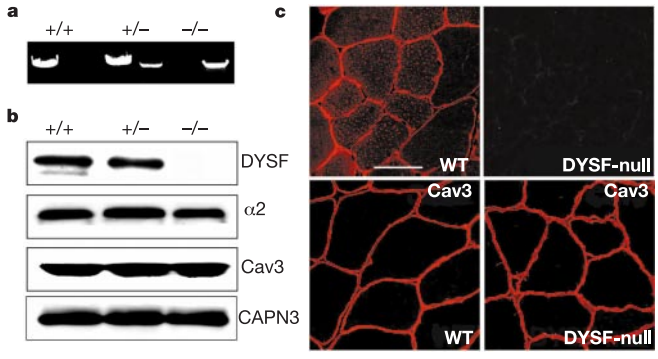

Figure 1 Complete loss of dysferlin expression in dysferlin-null mice. **a**, PCR genotyping of the wild-type (+/+), heterozygous (+/−) and dysferlin-null (−/−) mice. **b**, Loss of dysferlin (DYSF) expression by western blot analysis. Expression analysis of caveolin-3 (Cav3) and calpain 3 (CAPN3) and α2 (calcium channel subunit, for equal loading control). **c**, Immunofluorescence staining for dysferlin on skeletal muscle shows sarcolemma and vesicular cytoplasmic staining in wild-type muscle (WT) but a complete loss of staining in dysferlin-null (DYSF-null) muscle. Lower panels, normal staining for caveolin-3 in WT and DYSF-null skeletal muscle. Scale bar, 50 μm.

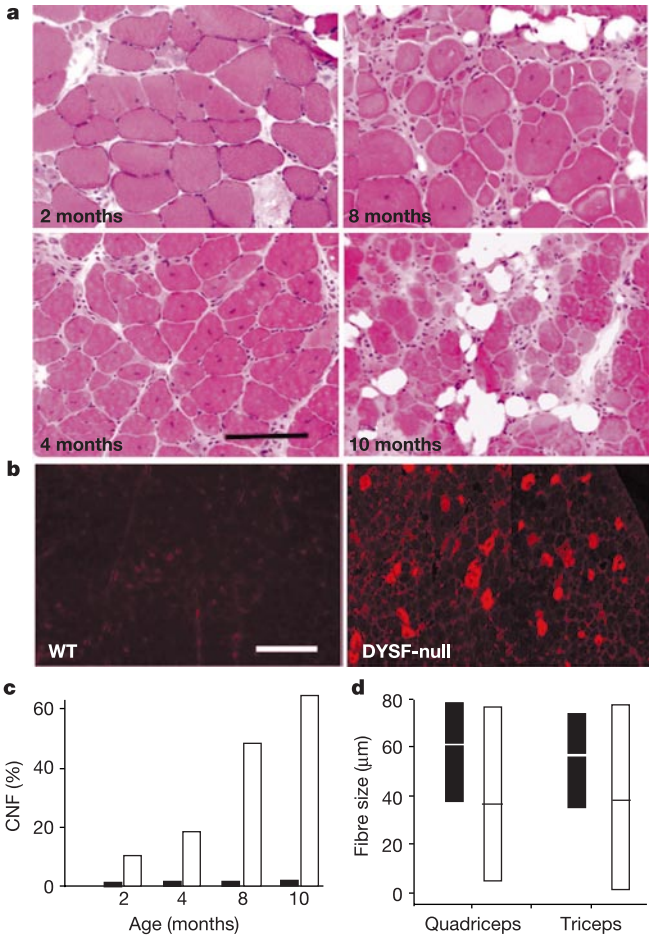

Figure 2 Dysferlin-null mice develop progressive muscular dystrophy. **a**, Haematoxylin–eosin-stained dysferlin-null skeletal muscle (quadriceps muscle) sections at 2, 4, 8 and 10 months of age. Scale bar, 100 μm. **b**, Individual Evans-blue-positive fibres can be detected in dysferlin-null (DYSF-null) muscle (9-month-old mice) but not in wild-type muscle (WT). Scale bar, 150 μm. **c**, Percentage of centrally nucleated fibres (CNF) increases with age in dysferlin-null muscle (open bars) but not in WT muscle (filled bars). For each sample set, $n > 1{,}000$; the data shown are an average of three sample sets. **d**, Greater fibre size variation was observed in dysferlin-null muscle (open bars) than in WT muscle (filled bars). The central horizontal line in each bar is the fibre diameter mean, and the size of each box is the size variation; $n = 3$ or 4 muscles from 9-month-old mice, with a total of 500–700 fibres.

© 2003 Nature Publishing Group

nucleated fibres in wild-type mice never exceeded 2%. A much greater fibre size variability was also observed in dysferlin-null skeletal muscle than in wild-type muscle (Fig. 2d).

Several types of muscular dystrophy are linked to components of the DGC[1,10]. In the DGC-linked muscular dystrophies, mutation in one of the DGC components disrupts the stability of the whole complex at the sarcolemma[9,11], which in turn disrupts the structural link between the sub-sarcolemma cytoskeleton and the extracellular matrix leading to an unstable sarcolemma. Disruption of this link makes the muscle more susceptible to contraction-induced injuries[1,12,13]. To test whether the loss of dysferlin has any effect on the stability of DGC components, the expression of various DGC components was evaluated by immunofluorescence (Fig. 3a) and western blot analysis on KCl-washed skeletal muscle membranes (Fig. 3b). However, no change was observed in the expression of the DGC components in dysferlin-null muscle. Furthermore, biochemical purification of the DGC from skeletal muscle also suggests the presence of a stable and functional DGC in dysferlin-null mice (Supplementary Fig. 3). We further tested the structural stability of the sarcolemma by exercising wild-type, dysferlin-null and mdx mice downhill on a treadmill[14] (−10° angle) for 30 min at a speed of 25 m min^{-1}. A comparison of Evans blue uptake and serum creatine kinase levels, before and after running, was used as a measure for the sarcolemma damage. The mdx mice have a mutation in the *dystrophin* gene[10], which causes disruption of the DGC and an unstable sarcolemma. This form of exercise, as expected, caused extensive membrane damage in the muscle of mdx mice, reflected by the significant increase in the serum creatine kinase levels and Evans blue uptake after exercise. By contrast, minimal damage was observed in wild-type and dysferlin-null mice, suggesting the presence of a stable sarcolemma in dysferlin-null mice (Fig. 3c). Taken together, these results suggest that the dysferlin-null mice have a functional DGC and that the mechanism of muscle degeneration in LGMD2B and Miyoshi myopathy patients is different from the DGC-linked muscular dystrophies.

Mechanical stress can cause muscle fibre necrosis by two separate mechanisms. First, as already mentioned, the sarcolemma of a muscle fibre could be more susceptible to injury, as in DGC-linked muscular dystrophies. Second, a muscle fibre could have a defective sarcolemma repair mechanism. Because the sarcolemma is structurally stable in dysferlin-null muscle, we propose that dysferlin has a role in the sarcolemma repair process. Membrane repair is a basic cellular mechanism that is required to reseal plasma membrane disruptions. Because plasma membrane disruption is a physiological event in skeletal muscle[13,15], the result of defective repair would be muscle fibre degeneration. Previous studies showed that membrane repair requires the accumulation and fusion of vesicles near the site of membrane disruptions[16–19]. Electron microscopic analysis of dysferlin-null muscle revealed sites of sarcolemma disruption associated with underlying accumulations of vesicles (Fig. 4a).

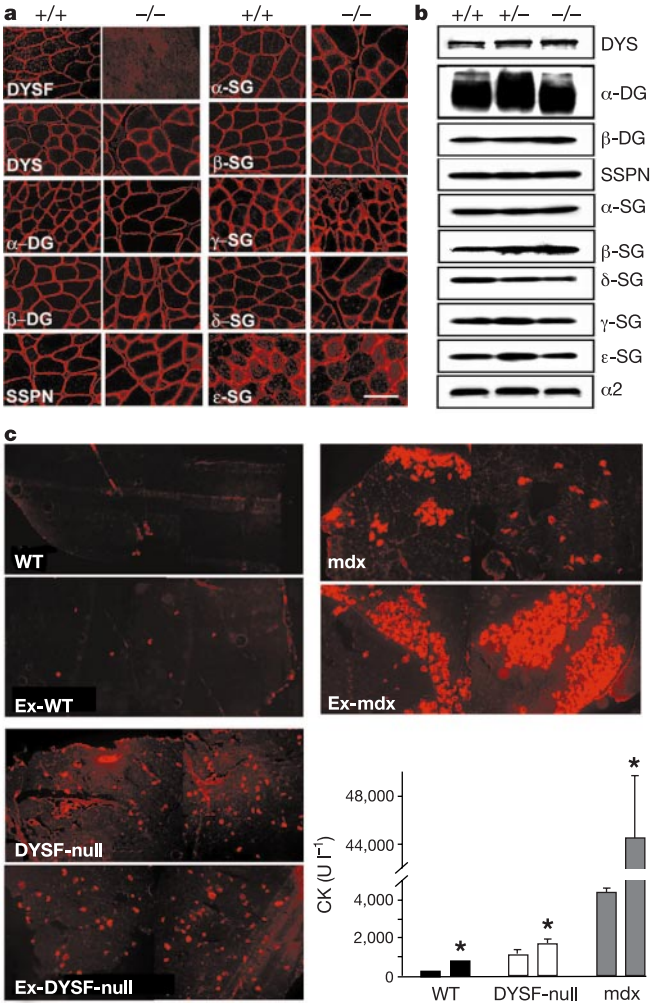

Figure 3 Normal expression of DGC components and a structurally stable sarcolemma in dysferlin-null mice. **a**, No staining for dysferlin (DYSF) but normal immunofluorescence of dystrophin (DYS), α-dystroglycan (α-DG), β-dystroglycan (β-DG), α-sarcoglycan (α-SG), β-sarcoglycan (β-SG), δ-sarcoglycan (δ-SG), γ-sarcoglycan (γ-SG), ε-sarcoglycan (ε-SG) and sarcospan (SSPN) in dysferlin-null muscle. Scale bar, 100 μm. **b**, Western blotting shows normal expression of DGC components in dysferlin-null mice; α2 used as a loading control. **c**, Significant increase in Evans blue uptake and serum creatine kinase (CK) levels was observed after exercise in mdx mice but not in wild-type (WT) and dysferlin-null (DYSF-null) mice ($n = 5$). Vertical bars (asterisks) are creatine kinase levels after exercise. Data are means ± s.d.

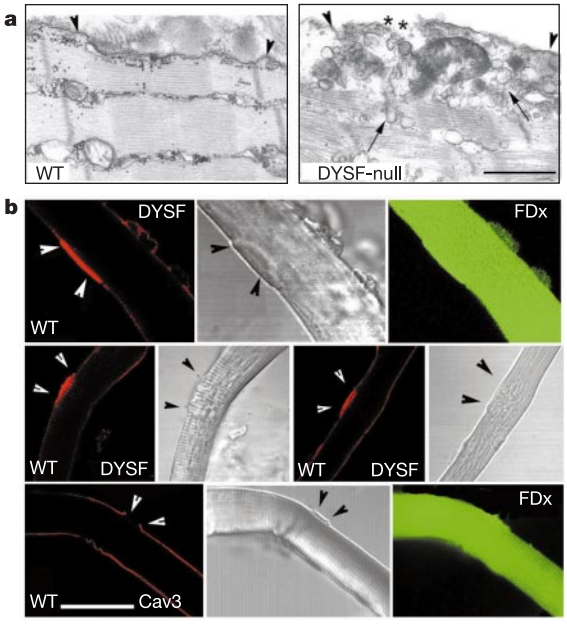

Figure 4 Vesicle accumulation and dysferlin-enriched membrane patches on the damaged muscle fibres. **a**, Electron micrograph of wild-type (WT) and dysferlin-null (DYSF-null) skeletal muscle. Sites with disrupted sarcolemma (asterisks) and vesicle accumulation (arrows) below the membrane (arrowheads) could be detected only in dysferlin-null muscle. Scale bar, 1 μm. **b**, Top two rows, membrane patches and wounds (bright field, arrowhead) enriched in dysferlin could be detected on the WT damaged fibres (positive for fluorescein dextran (FDx)). Bottom row, loss of caveolin-3 (Cav3) staining at the membrane patch sites was observed. Scale bar, 50 μm.

© 2003 Nature Publishing Group

Similar morphologies were not detected in wild-type muscle. This result and several other observations, such as the homology of dysferlin to FER-1 in *C. elegans* (which has a role in vesicle fusion to the plasma membrane), the presence of six C2 domains in dysferlin, and a protein structure similar to that of synaptotagmins, are consistent with our hypothesis that dysferlin functions in plasma membrane repair. Synaptotagmins are a family of proteins with a role in vesicle trafficking and fusion to the plasma membrane, and regulate important cellular events including membrane repair in certain cell types[20]. Moreover, the first C2 domain of dysferlin binds to phospholipids in a Ca^{2+}-dependent manner[21].

To evaluate the role of dysferlin in membrane repair, dysferlin distribution was analysed in damaged single muscle fibres isolated from wild-type mice. Muscle fibres were damaged in the presence of a membrane-impermeant fluorescein dextran (FDx) to mark those fibres that experienced membrane damage. Dysferlin distribution was analysed by immunofluorescence on permeabilized fibres. The undamaged fibres (FDx-negative) showed intact sarcolemma and uniform membrane staining of dysferlin (not shown). Membrane wounds and patches of various sizes were detected (Fig. 4b, bright field) on the damaged fibres (FDx-positive). Interestingly, immunofluorescence analysis revealed the enrichment of dysferlin in these patches (Fig. 4b, arrowheads in top two rows). According to the 'patch hypothesis'[22], membrane repair requires the accumulation and fusion of vesicle populations with each other and with the plasma membrane at or near the disruption. A 'patch' is thereby added across a defect, resealing the disrupted membrane[16]. Proteins with a direct role in this process can be detected at the disruption sites[17,20]. We suggest that these dysferlin-enriched membrane patches correspond to the membrane wound sites on the damaged muscle fibres. To confirm this, we stained damaged fibres with the known sarcolemma proteins such as caveolin-3 (Fig. 4b, bottom row) and δ-sarcoglycan[1,14] (not shown). A membrane disruption would cause a transient loss and reduction of the sarcolemma proteins at the wound sites. We detected a range from reduced staining to complete loss of these sarcolemma markers on the patch sites, confirming that these are indeed the wound sites on the sarcolemma. Our demonstration of dysferlin enrichment on the membrane disruption sites therefore strongly suggests a direct role of dysferlin in the membrane repair process.

To explore this potential mechanism further, a membrane repair assay was used[23] in a direct assessment of the resealing efficiency of dysferlin-null muscle. This assay was performed on single muscle fibres isolated from the flexor digitorum brevis muscle of the dysferlin-null and wild-type mice. Muscle fibres were irradiated with the mode-locked laser of a two-photon confocal scanning microscope to create plasma membrane disruptions. This injury was performed in the presence of FM 1-43, a membrane-impermeant fluorescent dye. FM 1-43 is soluble in both water and lipid, does not cross intact bilayers, and fluoresces only in lipidic environments such as cell membranes. At steady state, therefore, the membrane fluorescence of a wounded, unresealed muscle fibre will increase many-fold owing to the presence of endo-membrane that becomes stained with the dye. Resealing of the membrane halts this increase in fluorescence. The fluorescence that developed near the disruption (laser irradiation) site was imaged and measured at 10-s intervals beginning 20 s before ($t = 0$) and extending until about 3 min after the damage was induced. The initial fluorescence intensity (before the damage was induced) was set to 0 and the values show the increase in fluorescence intensity after the damage was induced. Wild-type muscle fibres, damaged in the presence of Ca^{2+}, significantly impeded further dye entry at about the 1-min time point after disruption (Fig. 5a, uppermost row of panels, and Fig. 5b, filled circles), suggesting that, on average, these fibres resealed within 1 min in the presence of Ca^{2+}. In contrast, wild-type fibres damaged in the absence of Ca^{2+} displayed comparatively little ability to impede dye entry over the entire time course of the experiment, suggesting a failure of resealing (Fig. 5a, second row of panels, and Fig. 5c, filled circles). This result suggests that muscle fibres can reseal their membrane efficiently and that membrane resealing is a Ca^{2+}-dependent process in skeletal muscle similar to that in many other cell types. Interestingly, dysferlin-null fibres in the presence of Ca^{2+} failed to halt dye uptake after an identical laser-induced disruption was created (Fig. 5a, third row of panels, and Fig. 5b, open triangles). Indeed, the apparently unimpeded uptake of FM 1-43 observed in dysferlin-null fibres in the presence of Ca^{2+} was similar to that observed in the wild-type and dysferlin-null (Fig. 5a, bottom row of panels, and Fig. 5c, open triangles) experiments conducted in the absence of resealing-permissive Ca^{2+}. Unlike dysferlin-null fibres, membrane repair assays conducted on muscle fibres in mdx mice showed efficient membrane resealing in the presence of Ca^{2+} similar to that in wild-type muscle (P. McNeil, personal communication). These results indicate that dysferlin-null muscle fibres are defective in Ca^{2+}-dependent resealing of sarcolemma disruptions.

We suggest that dysferlin has a role during the membrane fusion step of the repair process in muscle fibres. Such a role is consistent with the presence of several C2 domains in dysferlin and with its homology to several known proteins with a role in vesicle fusion. We propose that dysferlin, present on the vesicles, facilitates vesicle docking and fusion with the plasma membrane either by interacting

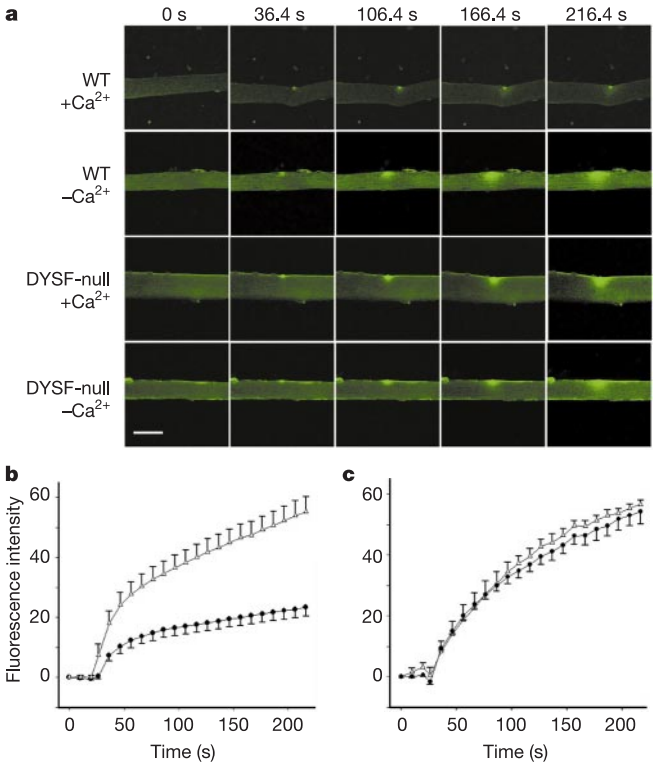

Figure 5 Defective resealing of membranes in dysferlin-null muscle. **a**, Membrane repair assay performed on wild-type (WT) and dysferlin-null (DYSF-null) single muscle fibres in the presence and absence of Ca^{2+}. The damage was induced at $t = 20$ s. The top two rows of panels show the assay performed on wild-type fibres in the presence (WT + Ca^{2+}) and absence (WT − Ca^{2+}) of Ca^{2+}. The bottom two rows of panels show the repair assay performed on dysferlin-null fibres in the presence (DYSF-null + Ca^{2+}) and absence (DYSF-null − Ca^{2+}) of Ca^{2+}. Scale bar, 50 μm. **b**, Plot of fluorescence intensity ($n = 16$) against time in WT (filled circles) and dysferlin-null (open triangles) fibres in the presence of Ca^{2+}. Data are means ± s.e. **c**, Measurement of fluorescence intensity ($n = 4$) versus time in WT (filled circles) and dysferlin-null (open triangles) fibres in the absence of Ca^{2+}. Data are means ± s.e.; statistical analysis was done with Student's *t*-test. $P < 0.05$ is considered significant.

© 2003 Nature Publishing Group

with the other dysferlin molecules or with some other unknown protein-binding partner(s) at the plasma membrane.

The finding that dysferlin-null muscle is inefficient in plasma membrane resealing highlights the importance of this basic cellular function in various forms of muscular dystrophy. Because cell membrane repair is required for surviving a mechanical injury, and given that cell wounding is common in many mechanically active mammalian cells, defects in this repair pathway may be linked to other human diseases. This study reveals a novel mechanism of muscular dystrophy in which the membrane repair machinery of muscle is defective, as opposed to several other types of muscular dystrophies in which the primary defect is in the stability of sarcolemma. Dysferlin is the first identified member of the membrane repair machinery in skeletal muscle. This finding will help to identify other members of the muscle membrane repair machinery, and those will serve as potential candidate genes for other muscular dystrophies and muscle-related diseases with unknown aetiology. □

Methods

Generation of dysferlin-null mice

The targeting vector was constructed to delete the last three coding exons including the exons coding for the transmembrane domain of the dysferlin gene. The targeting vector was electroporated into R1 embryonic stem cells, and clones carrying the specific targeted locus were confirmed by PCR screening and sequencing of the PCR product. Targeted clones were used to generate chimaeric mice by blastocyst injections. Heterozygous mice obtained from the chimaeric mice were bred together to obtain homozygous mutant mice. Homozygous mutant mice were backcrossed with C57/BL6 wild-type mice for two generations. Wild-type littermates were used as controls. Dysferlin-null mice are viable and have a normal growth rate.

Membrane repair assay

This experiment was performed on four wild-type and four dysferlin-null mice at 6 weeks of age, blind to the genotype. For every mouse, the assay was performed on four different fibres in the presence of Ca^{2+} and one or two fibres in the absence of Ca^{2+}. Single muscle fibres were isolated from the flexor digitorum brevis muscle by treatment with collagenase I. Fibres were washed and resuspended in Dulbecco's PBS containing 1 mM Ca^{2+} (Gibco) for the resealing experiment in the presence of Ca^{2+}, and PBS containing 1 mM EGTA for the resealing experiment in the absence of Ca^{2+}. Single fibres were mounted on a glass slide chamber and membrane damage was induced in the presence of FM 1-43 dye (2.5 μM; Molecular Probes) with a two-photon confocal laser-scanning microscope (LSM 510; Zeiss) coupled to a 10-W Argon/Ti:sapphire laser[23]. To induce damage, a 5 μm × 5 μm area of the sarcolemma on the surface of the muscle fibre was irradiated at full power for 6.4 s at $t = 20$ s. Images were captured beginning 20 s before ($t = 0$) and for 3 min after the irradiation at 10-s intervals. For every image taken, the fluorescence intensity at the site of the damage was measured with the Zeiss LSM 510 imaging software. Fibres that had no membrane resealing showed dye filling at the wound site over the entire course of the experiment, whereas dye influx halted within 1 min for the fibres that resealed under the experimental conditions.

Analysis of dysferlin expression on damaged muscle fibres

Single muscle fibres were damaged by being flushed through an 18-gauge syringe in the presence of lysine-fixable fluorescein dextran dye (10 kDa, 10 mg ml^{-1} in PBS; Molecular Probes). After incubation for 2 min at 37 °C, fibres were transferred to ice, washed with chilled PBS and fixed in 4% paraformaldehyde for 10 min. Fibres were then washed with PBS and permeabilized with detergent; immunofluorescence analysis was performed with antibodies against dysferlin, caveolin-3 and δ-sarcoglycan. Dysferlin, caveolin-3 and δ-sarcoglycan distribution was analysed on more than 200 damaged muscle fibres: 25 fibres showed dysferlin-enriched sites, but none of them showed any kind of membrane enrichment for caveolin-3 or δ-sarcoglycan.

Biochemical, immunofluorescence and histological analysis

KCl-washed skeletal muscle membranes were prepared and western blot analysis was performed as described previously[24,25]. DGC purification from the total muscle homogenates was performed as described previously[25]. Western blot analysis of dysferlin was performed using an amino-terminal rabbit polyclonal antibody. Rabbit polyclonal antibody against mouse dysferlin was generated by injecting New Zealand white rabbits intramuscularly and subcutaneously with an N-terminal dysferlin peptide (LLADCSQPLCDIHEIPSATH; single-letter amino acid codes). Antibody specificity was verified by competition experiments with the corresponding peptide on the western blot. Antibodies against DGC components were used as described previously[9,14]. Expression analysis of caveolin-3 and calpain 3 was performed with mouse monoclonal antibodies; caveolin-3 (Transduction Laboratories) and calpain 3 (Calp3c12A2; Novocastra). Immunofluorescence was performed on 7-μm transverse cryosections as described previously[9]. For dysferlin immunostaining, the monoclonal antibody Hamlet (Novocastra)[26] was used at 1:25 dilution with an *in situ* antigen denaturation method described previously[27]. One-year-old dysferlin-null and wild-type mice were perfused with 2% paraformaldehyde in PBS and quadriceps muscle was dissected out for electron microscopic analysis. Tissue processing was done as described previously[5]. Histological analysis of skeletal muscle and Evans blue injections and exercise experiments were performed as described previously[8,9,14].

Received 27 December 2002; accepted 14 March 2003; doi:10.1038/nature01573.

1. Cohn, R. D. & Campbell, K. P. Molecular basis of muscular dystrophies. *Muscle Nerve* **23,** 1456–1471 (2000).
2. Bashir, R. *et al.* A gene related to *Caenorhabditis elegans* spermatogenesis factor *fer-1* is mutated in limb-girdle muscular dystrophy type 2B. *Nature Genet.* **20,** 37–42 (1998).
3. Liu, J. *et al.* Dysferlin, a novel skeletal muscle gene, is mutated in Miyoshi myopathy and limb girdle muscular dystrophy. *Nature Genet.* **20,** 31–36 (1998).
4. Achanzar, W. E. & Ward, S. A nematode gene required for sperm vesicle fusion. *J. Cell Sci.* **110,** 1073–1081 (1997).
5. Piccolo, F., Moore, S. A., Ford, G. C. & Campbell, K. P. Intracellular accumulation and reduced sarcolemmal expression of dysferlin in limb-girdle muscular dystrophies. *Ann. Neurol.* **48,** 902–912 (2000).
6. Matsuda, C. *et al.* The sarcolemmal proteins dysferlin and caveolin-3 interact in skeletal muscle. *Hum. Mol. Genet.* **10,** 1761–1766 (2001).
7. Anderson, L. V. *et al.* Secondary reduction in calpain 3 expression in patients with limb girdle muscular dystrophy type 2B and Miyoshi myopathy (primary dysferlinopathies). *Neuromusc. Disord.* **10,** 553–559 (2000).
8. Straub, V., Rafael, J. A., Chamberlain, J. S. & Campbell, K. P. Animal models for muscular dystrophy show different patterns of sarcolemmal disruption. *J. Cell Biol.* **139,** 375–385 (1997).
9. Duclos, F. *et al.* Progressive muscular dystrophy in α-sarcoglycan-deficient mice. *J. Cell Biol.* **142,** 1461–1471 (1998).
10. Durbeej, M. & Campbell, K. P. Muscular dystrophies involving the dystrophin–glycoprotein complex: an overview of current mouse models. *Curr. Opin. Genet. Dev.* **12,** 349–361 (2002).
11. Ervasti, J. M., Ohlendieck, K., Kahl, S. D., Gaver, M. G. & Campbell, K. P. Deficiency of a glycoprotein component of the dystrophin complex in dystrophic muscle. *Nature* **345,** 315–319 (1990).
12. Petrof, B. J., Shrager, J. B., Stedman, H. H., Kelly, A. M. & Sweeney, H. L. Dystrophin protects the sarcolemma from stresses developed during muscle contraction. *Proc. Natl Acad. Sci. USA* **90,** 3710–3714 (1993).
13. Clarke, M. S., Khakee, R. & McNeil, P. L. Loss of cytoplasmic basic fibroblast growth factor from physiologically wounded myofibers of normal and dystrophic muscle. *J. Cell Sci.* **106,** 121–133 (1993).
14. Coral-Vazquez, R. *et al.* Disruption of the sarcoglycan–sarcospan complex in vascular smooth muscle: a novel mechanism for cardiomyopathy and muscular dystrophy. *Cell* **98,** 465–474 (1999).
15. McNeil, P. L. & Khakee, R. Disruptions of muscle fiber plasma membranes. Role in exercise-induced damage. *Am. J. Pathol.* **140,** 1097–1109 (1992).
16. McNeil, P. L. & Terasaki, M. Coping with the inevitable: how cells repair a torn surface membrane. *Nature Cell Biol.* **3,** E124–E129 (2001).
17. Bi, G. Q., Alderton, J. M. & Steinhardt, R. A. Calcium-regulated exocytosis is required for cell membrane resealing. *J. Cell Biol.* **131,** 1747–1758 (1995).
18. Miyake, K. & McNeil, P. L. Vesicle accumulation and exocytosis at sites of plasma membrane disruption. *J. Cell Biol.* **131,** 1737–1745 (1995).
19. Steinhardt, R. A., Bi, G. & Alderton, J. M. Cell membrane resealing by a vesicular mechanism similar to neurotransmitter release. *Science* **263,** 390–393 (1994).
20. Reddy, A., Caler, E. V. & Andrews, N. W. Plasma membrane repair is mediated by Ca^{2+}-regulated exocytosis of lysosomes. *Cell* **106,** 157–169 (2001).
21. Davis, D. B., Doherty, K. R., Delmonte, A. J. & McNally, E. M. Calcium-sensitive phospholipid binding properties of normal and mutant ferlin C2 domains. *J. Biol. Chem.* **277,** 22883–22888 (2002).
22. McNeil, P. L., Vogel, S. S., Miyake, K. & Terasaki, M. Patching plasma membrane disruptions with cytoplasmic membrane. *J. Cell Sci.* **113,** 1891–1902 (2000).
23. McNeil, P. L., Miyake, K. & Vogel, S. S. The self-sealing membrane concept. *Proc. Natl Acad. Sci. USA* **100,** 4592–4597 (2003).
24. Ohlendieck, K. & Campbell, K. P. Dystrophin-associated proteins are greatly reduced in skeletal muscle from mdx mice. *J. Cell Biol.* **115,** 1685–1694 (1991).
25. Durbeej, M. *et al.* Disruption of the β-sarcoglycan gene reveals pathogenetic complexity of limb-girdle muscular dystrophy type 2E. *Mol. Cell* **5,** 141–151 (2000).
26. Anderson, L. V. *et al.* Dysferlin is a plasma membrane protein and is expressed early in human development. *Hum. Mol. Genet.* **8,** 855–861 (1999).
27. Miner, J. H. *et al.* The laminin alpha chains: expression, developmental transitions, and chromosomal locations of α1-5, identification of heterotrimeric laminins 8–11, and cloning of a novel α3 isoform. *J. Cell Biol.* **137,** 685–701 (1997).

Supplementary Information accompanies the paper on **www.nature.com/nature**.

Acknowledgements We thank all members of the Campbell laboratory for the critical reading of this manuscript, discussions and supplying critical reagents; and M. Hassebrock, S. Lowen, E. Hurst and K. Garringer for technical assistance. D. Bansal was supported by American Heart Predoctoral Fellowship (Heartland). We thank the University of Iowa DNA Core Facility, which is supported in part by the Diabetes Endocrinology Research Center and the University of Iowa Roy J. and Lucille A. Carver College of Medicine. We also thank University of Iowa Central Microscopy Research Facility and the Medical College of Georgia Imaging Core. This work was supported by the Muscular Dystrophy Association (K.P.C.). P.L.McN. is supported by NASA, and S.S.V. by NIH. K.P.C. is an investigator of the Howard Hughes Medical Institute.

Competing interests statement The authors declare that they have no competing financial interests.

Correspondence and requests for materials should be addressed to K.P.C. (kevin-campbell@uiowa.edu).

© 2003 Nature Publishing Group